

Short Communication

Acetalization of Heptanal over Al-SBA-1 molecular sieve

K. Venkatachalam, M. Palanichamy, V. Murugesan*

Department of Chemistry, Anna University, Chennai 600 025, India

ARTICLE INFO

Article history:

Received 12 June 2010

Received in revised form 14 September 2010

Accepted 16 September 2010

Available online 21 September 2010

Keywords:

SBA-1

Acetalization

Hemiacetal

Acetal

Vinyl ether

ABSTRACT

Al-SBA-1 (Si/Al = 40, 80 and 120) and Al,Mg-SBA-1 (Si/(Al + Mg) = 40 and 80) molecular sieves were synthesized and characterized. Acetalization of *n*-heptanal with methanol was studied under autogenous pressure between 80 and 150 °C. Since protonation of *n*-heptanal was fast, addition of methanol to the same formed hemiacetal slowly whereas conversion of hemiacetal to acetal was fast. The catalysts exhibited nearly similar conversion irrespective of their difference in acidity, and all of them showed more than 80% conversion either at 80 or 100 °C. Hence, it is evident that the difference in acidity is not so important in differentiating the activity of the catalysts. The large pore size and hydrophilic and hydrophobic properties are suggested to be the main factors that control acetalization.

© 2010 Elsevier B.V. All rights reserved.

1. Introduction

The development of one-pot preparative procedure offers significant advantages due to reduction in the number of synthetic steps, significant increase in efficiency and prevention of isolation of intermediates [1]. Acetalization is a one-pot process and it is a specific requirement to protect the carbonyl group during manipulation of multifunctional organic molecules, since the product acetals display higher stability towards strong bases, Grignard reagents, lithium aluminium hydride, strong oxidants and esterification reagents than their parent carbonyl compounds [2]. Besides the interest of acetals as protecting groups, many of them found direct applications in fragrances and cosmetics [3,4], as food and beverage additives [5,6] and in the synthesis of enantiomerically pure compounds [7,8], steroids [9], pharmaceuticals [3,10] and polymers [11]. Since their demand is high in the market, mild and eco-friendly acetalization procedures with selective catalysts are important for acetalization. Traditionally, acetalization of aldehydes and ketones is performed using trimethyl orthophosphate in the presence of acid catalysts such as HCl, H₂SO₄, *p*-toluene sulphonic acid and ferric chloride [12,13]. Eco-friendly solid acid catalysts such as sulphated zirconia and titania [14], Ce-exchanged Montmorillonite clay [15], acidic zeolites [3,16,17] and siliceous mesoporous materials [18] were also reported to be active for acetalization. One-pot acetalization of cyclohexanone, acetophenone and benzophenone was carried out using methanol over H-montmorillonite clay, silica, alumina and

different zeolites such as HY, H β , HZSM-5 and HMOR by Thomas et al. [19]. But zeolites exhibited mass transport limitations.

Mesoporous solid acid catalysts are advantageous as they are non-hazardous and free from mass transport limitations, possess high surface area and provide easy catalyst recovery. Based on the advantages of mesoporous materials, acetalization of *n*-heptanal with methanol was attempted for the first time over SBA-1 molecular sieves. The product, acetal, is used as a flavouring agent for beverages, chewing gum and cordimonts. Acetalization of *n*-heptanal has not been reported so far over solid acid catalysts in general and SBA-1 in particular.

2. Experimental

2.1. Preparation of the catalysts

Al-SBA-1 molecular sieves were synthesized under acidic conditions using cetyltriethylammonium bromide as the template. Tetraethyl orthosilicate (TEOS, Aldrich, 98%) and aluminium hydroxide were used in aqueous solution of hydrochloric acid (4.5 N) Cetyltriethylammonium bromide (CTEABr) was synthesized by reacting equimolar amount of 1-bromohexadecane and triethylamine in ethanol under reflux for 2 days. The resultant surfactant was purified by recrystallization with chloroform and ethyl acetate mixture [20].

Al-SBA-1 was synthesized as follows: solution "A" was prepared by adding CTEABr (2.46 g) to dil. HCl (4.5 N), cooled to 0 °C and homogenized for 30 min. The pre-cooled (0 °C) TEOS and aluminium hydroxide was then added to solution A under vigorous stirring which continued for 5 h at 0 °C. The mixture was then heated at 100 °C for 1 h. The solid product was recovered by filtration and dried in an oven overnight at 100 °C. The gel composition was: 1 TEOS: 0.0025–0.025

* Corresponding author. Tel.: +91 44 22357023/22358645; fax: +91 44 2220066/22201213.

E-mail address: v_murugu@hotmail.com (V. Murugesan).

Al(OH)₃: 0.2 CTEABr: 10–56 HCl: 125–700 H₂O. The as-synthesized material was calcined in air at 550 °C for 6 h. Al,Mg-SBA-1 (Si/(Al + Mg) = 40 and 80) molecular sieves were synthesized by adopting the same procedure. Magnesium acetate was used as the precursor for magnesium.

2.2. Characterization

The X-ray diffraction (XRD) patterns of calcined Al-SBA-1 and Al,Mg-SBA-1 catalysts were recorded on a PANalytical X'Pert Pro X-ray diffractometer using CuK α radiation. The low angle diffractograms were recorded in the 2 θ range 1.0–10° with a 2 θ step size of 0.01° and a step time of 10 s at each point. Surface area was measured by nitrogen adsorption at 77 K on a ASAP-2010 porosimeter from Micromeritics Corporation (Norcross, GA, USA). The density and strength of acid sites were determined by temperature programmed desorption of ammonia (TPD NH₃) on a Micromeritics chemisorb 2750 pulse chemisorption system. FT-IR spectra of the materials were recorded on a Nicolet (Avatar 360) FT-IR spectrometer. Scanning electron microscopic (SEM) images were obtained from a SEM (Hitachi S-4500LV) instrument.

2.3. Catalytic studies

A mixture of *n*-heptanal (1 mol), methanol (3 mol) and a freshly activated catalyst (0.05 g) was taken in a 50 ml autoclave. The autoclave was then placed in an oven and the temperature kept at 80, 100, 120 or 150 °C for 12 h. It was then cooled and the sample centrifuged. The centrifugate was analyzed with a gas chromatograph (Shimadzu GC-17A) using DB-5 capillary column (30 m \times 0.25 mm \times 0.25 μ m) equipped with a FID detector. The identification of products was also made using GC-MS Perkin Elmer Auto System XL gas chromatograph (Perkin-Elmer elite series PE-5 capillary column, 30 m \times 0.25 mm \times 1 μ m) equipped with a Turbo mass spectrometer (EI, 70 eV) with helium as carrier gas at a flow rate of 1 ml/min.

3. Results and discussion

3.1. XRD

The XRD patterns of Al-SBA-1 (Si/Al = 40, 80 and 120), Al,Mg-SBA-1 (Si/(Al + Mg) = 40 and 80) are shown in Fig. 1. Al-SBA-1 molecular sieves showed characteristic patterns corresponding to (200), (210) and (211) of a three-dimensional cubic structure (space group *Pm3n*).

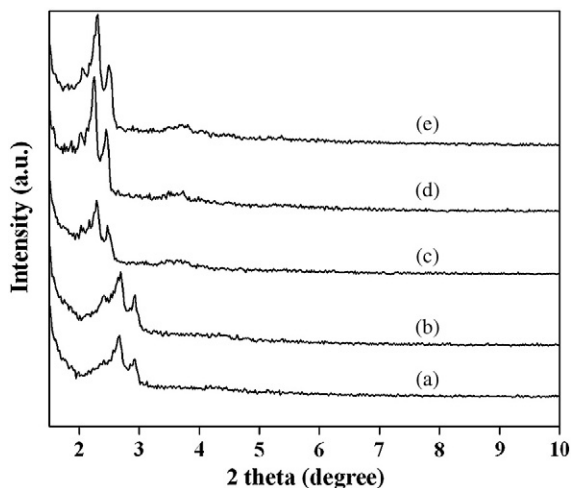


Fig. 1. XRD patterns of calcined (a) Al,Mg-SBA-1 (40), (b) Al,Mg-SBA-1 (80), (c) Al-SBA-1 (40), (d) Al-SBA-1 (80), and (e) Al-SBA-1 (120).

These patterns matched well with the previous reports [21,22]. However, the intensity of patterns decreased with increase in the Si/Al ratio. Hence, isomorphic substitution of silicon by aluminium is suggested to decrease the orderly arrangement of pores. The same observation was also noted in Al,Mg-SBA-1 catalysts. The intensity of the patterns of Al,Mg-SBA-1 (Si/(Al + Mg) = 40) was less than Al,Mg-SBA-1 (Si/(Al + Mg) = 80). In addition, the position of the patterns in both Al-SBA-1 and Al,Mg-SBA-1 are shifted to lower 2 θ with the decrease in aluminium content. Hence, the interplanar spacing of the planes might increase with a decrease in the aluminium content.

3.2. BET

The nitrogen adsorption-desorption isotherms of Al-SBA-1 (Si/Al = 40, 80 and 120), Al,Mg-SBA-1 (Si/(Al + Mg) = 40, and 80) are shown in Fig. 2. The isotherms are quite similar and a steep increase in all the isotherms due to pore condensation occurred below 0.1 (p/p_0) for all the samples. Similar isotherms were also reported by Dai et al., Che et al. and Balasubramanian et al. [23–25]. The pore condensation reached the maximum for Al-SBA-1 (40) close to relative pressure (p/p_0) of 0.2 whereas the same is shifted to relative pressure (p/p_0) of 0.3 for Al-SBA-1 (80) and Al-SBA-1 (120). Hence, the pore size of these catalysts is larger than Al-SBA-1 (40). Al,Mg-SBA-1 (Si/(Al + Mg) = 40 and 80) showed nearly similar p/p_0 values for pore condensation and the curves are nearly similar to Al-SBA-1 (40). Based on the smooth rise in pore condensation, it could be inferred that there may be uniform distribution of pores. The surface area varied from 1050 to 1360 m²/g and pore size from 2.48 to 2.78 nm (Table 1). Though the relative pressure for pore condensation is low, it cannot be presumed that materials are microporous. As the surface area and pore size are high and they show XRD patterns at low angles which are characteristics of mesoporous materials.

3.3. TPD—ammonia

The acidity of mesoporous materials was determined by TPD (NH₃) and the results are presented in Table 2. All the materials possess weak and medium acid sites, and this classification is mainly based on the desorption of ammonia between 150 and 250 °C for weak acid sites and 250 and 350 °C for medium acid sites. This is the common distribution observed for all mesoporous materials. There is no systematic variation of total acidity with the variation of Si/Al ratio. It is an indirect evidence for non-framework alumina in them. But further attempts were made to prove such non-framework species.

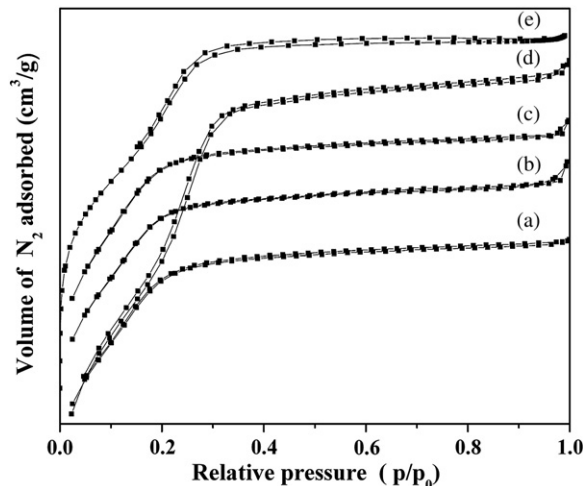


Fig. 2. Adsorption isotherms of (a) Al,Mg-SBA-1 (40), (b) Al,Mg-SBA-1 (80), (c) Al-SBA-1 (40), (d) Al-SBA-1 (80) and (e) Al-SBA-1 (120).

Table 1
Textural properties of the catalysts.

Catalyst	BET surface area (m ² /g)	Pore volume (cm ³ /g)	Pore size (nm)
Al-SBA-1 (40)	1220	0.70	2.56
Al-SBA-1 (80)	1305	0.73	2.75
Al-SBA-1 (120)	1360	0.74	2.78
Al,Mg-SBA-1 (40)	1050	0.67	2.53
Al,Mg-SBA-1 (80)	1230	0.71	2.48

3.4. FT-IR

The FT-IR spectra of calcined Al-SBA-1 (Si/Al = 40, 80 and 120), Al, Mg-SBA-1 (Si/(Al + Mg) = 40, and 80) are shown in Fig. 3. All the spectra showed similar features irrespective of aluminium or magnesium content. The presence of defective –OH groups in all the catalysts are confirmed by its stretching vibration, which occurred around 3740 cm⁻¹. The broad envelope between 3000 and 3740 cm⁻¹ is due to –OH stretching vibration of water. The broadening is due to hydrogen bonding. The asymmetric stretching vibrations of Si-O-Si and Si-O-Al (or Mg) bonds gave intense broad bands between 1000 and 1300 cm⁻¹. Their bending modes occurred just below 1000 cm⁻¹. The –OH stretching vibrations of water in all the spectra were broad and intense, indicating significant hydrophilic property.

3.5. SEM

The SEM image of Al-SBA-1 (40) is shown in Fig. 4. Most of the particles revealed spherical morphology with different size, but larger particles dominated over smaller particles. These larger particles have a size range of 250–400 nm. Similar features were also shown by the images of other molecular sieves (figure not shown). But the size of the particles is slightly smaller than that of Fig. 4. The morphology of the particles is nearly same as that reported earlier [25].

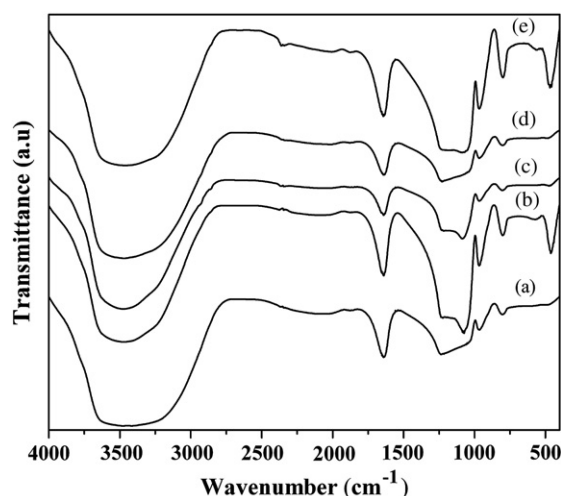
3.6. Catalytic studies

3.6.1. Effect of temperature

The results of acetalization over Al-SBA-1 (Si/Al = 40, 80 and 120) and Al,Mg-SBA-1 (Si/(Al + Mg) = 40, 80) are presented in Table 3. The major products were hemiacetal, acetal, and vinyl ether. The *n*-heptanal conversion was less than 50% when the reaction was carried out in the liquid phase at 1 atm. below the boiling point of methanol (64.7 °C). Hence, the reaction was carried out under autogenous pressure and above the boiling point of methanol. The *n*-heptanal conversion decreased with the increase in temperature over each of the catalysts. Hence, high temperatures well above the boiling point of methanol are not favored for this reaction. Either the chemisorption of *n*-heptanal on the Bronsted acid sites or diffusion of methanol from the vapour phase into the liquid phase and into the mesopores where the chemisorbed *n*-heptanal available might be suppressed with the increase in temperature in order to show decrease in conversion with the increase in temperature. Among Al-

Table 2
Acidity data of Al-SBA-1 catalysts with different Si/Al and Si/(Al + Mg) ratios.

Catalyst	Acid sites (mmol/g)	
	Weak (150–250 °C)	Medium (250–350 °C)
Al-SBA-1 (40)	0.38	0.08
Al-SBA-1 (80)	0.20	0.05
Al-SBA-1 (120)	0.09	0.04
Al,Mg-SBA-1 (40)	0.42	0.12
Al,Mg-SBA-1 (80)	0.30	0.05

**Fig. 3.** FT-IR spectra of calcined (a) Al,Mg-SBA-1 (40), (b) Al,Mg-SBA-1 (80), (c) Al-SBA-1 (40), (d) Al-SBA-1 (80) and (e) Al-SBA-1 (120).

SBA-1 catalysts, Al-SBA-1 (40) showed higher conversion than the others. But the difference between the conversion of Al-SBA-1 (Si/Al = 40, 80 and 120) catalysts is not significant. Hence the acidity of the catalysts alone is not the important factor to account for their activity. Similar results were also reported by Rabindran Jermy et al. [26] for acetalization of cyclohexanone with different alcohols over Al-MCM-41 materials. Obviously, the hydrophilic and hydrophobic properties of the catalysts may play a prominent role in acetalization. Hence, Al-SBA-1 (80) and Al-SBA-1 (120) with low acidity and high hydrophobic property in comparison to Al-SBA-1 (40) can better adsorb hydrophobic *n*-heptanal than Al-SBA-1 (40) in order to exhibit high conversion. The hydrophobicity of the catalysts decreases in the order: Al-SBA-1 (40) < Al-SBA-1 (80) < Al-SBA-1 (120). This order is based on the Si/Al ratio of the catalysts. The intensity of –OH stretching vibration of water around 3400 cm⁻¹ and its bending vibration at about 1600 cm⁻¹ could be used for the comparison of hydrophilic and hydrophobic property of the catalysts. However, same amount of catalysts was not used for comparison.

The *n*-heptanal conversion over Al,Mg-SBA-1 also exhibited similar trends as that of Al-SBA-1 catalysts. The *n*-heptanal conversion decreased with increase in temperature, and both the catalysts showed nearly similar conversion. Hence, a slight increase in the acidity of Al-SBA-1 (40) may be compensated by a slight increase in hydrophobicity of Al-SBA-1 (80) in order to exhibit nearly similar conversion. Although these catalysts possess more density of acid sites than the corresponding Al-SBA-1 catalysts, nearly similar conversion of *n*-heptanal indicates that slightly high hydrophobicity

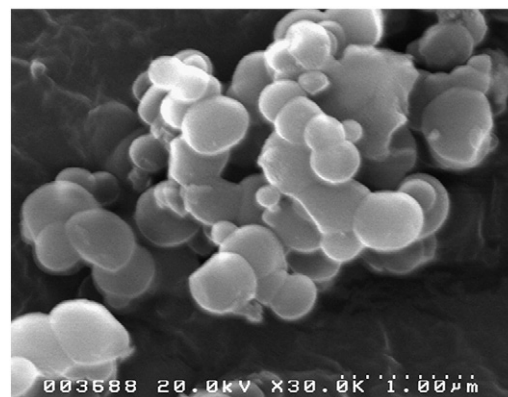
**Fig. 4.** SEM images of Al-SBA-1 (40).

Table 3
Effect of temperature on *n*-heptanal conversion and product selectivity.

Catalyst	Temperature (°C)	<i>n</i> -Heptanal conversion (%)	Product selectivity (%)		
			Acetal	Hemiacetal	Vinyl ether
Al-SBA-1 (40)	80	95	84	11	5
	100	92	86	08	6
	120	90	72	28	-
	150	87	68	32	-
Al-SBA-1 (80)	80	93	80	14	6
	100	90	82	10	8
	120	88	73	27	-
	150	85	59	41	-
Al-SBA-1 (120)	80	88	69	24	7
	100	82	66	22	12
	120	76	61	39	-
	150	72	55	45	-
Al,Mg-SBA-1 (40)	80	96	71	23	6
	100	93	76	16	8
	120	91	69	31	-
	150	89	61	39	-
Al,Mg-SBA-1 (80)	80	94	67	39	4
	100	92	62	26	12
	120	90	57	43	-
	150	87	51	49	-

Reaction condition: catalysts amount 0.05 g; time 8 h; pressure autogenous pressure; reactor 50 ml autoclave; Feed ratio 1:3 (*n*-heptanal: methanol).

of the latter catalysts plays a predominant role in equalizing acetalization. It could be speculated that hydrophilic and hydrophobic property could be very important for microporous materials but not so for mesoporous materials. When the reactants freely diffuse through the mesopores, there may be less hydrophobic force than in zeolites. The free mass transport may also be considered as the main cause for almost equal conversion over all the catalysts in addition to hydrophobic force. Hence, the catalysts need not possess a very high density of acid sites for acetalization under the given set of conditions, provided there is no diffusional problem.

The selectivity of hemiacetal increased with an increase in temperature. Hence adsorption of hemiacetal on the acid sites may be hindered at high temperatures. At higher temperatures, the selectivity of hemiacetal increased with increase in the hydrophobicity of the catalysts. This observation supports our view that an increase in hydrophobicity of the catalysts partly suppressed the effect of temperature on adsorption. The selectivity of acetal decreased with an increase in temperature is in accordance with the increase in the selectivity of hemiacetal. The formation of vinyl ether was observed at 80 and 100 °C but not at high temperatures. When hemiacetal is protonated, two reactions are possible. After the formation of carbonium ion, it can react with methanol to yield acetal or undergo dehydration to form vinyl ether. The low selectivity of vinyl ether indicates that it is not much favored in comparison to the reaction of hemiacetal with methanol.

3.6.2. Effect of reaction time

In order to establish the sequence of steps involved in acetalization, the effect of reaction time on *n*-heptanal conversion and the products' selectivity was tested and the results are presented in Fig. 5a. The *n*-heptanal conversion increased with an increase in reaction time. The increase was significant up to 8 h. As the selectivity to hemiacetal is less, its formation must be a slow process. In other words, protonation of *n*-heptanal is a slow process. Similarly, the formation of vinyl ether is also a slow process. However, protonation of hemiacetal must be rapid as the selectivity of acetal was high at all reaction intervals.

3.6.3. Effect of feed ratio

The effect of feed ratio on *n*-heptanal conversion and the products' selectivity was studied and the results are presented in Fig. 5b. The

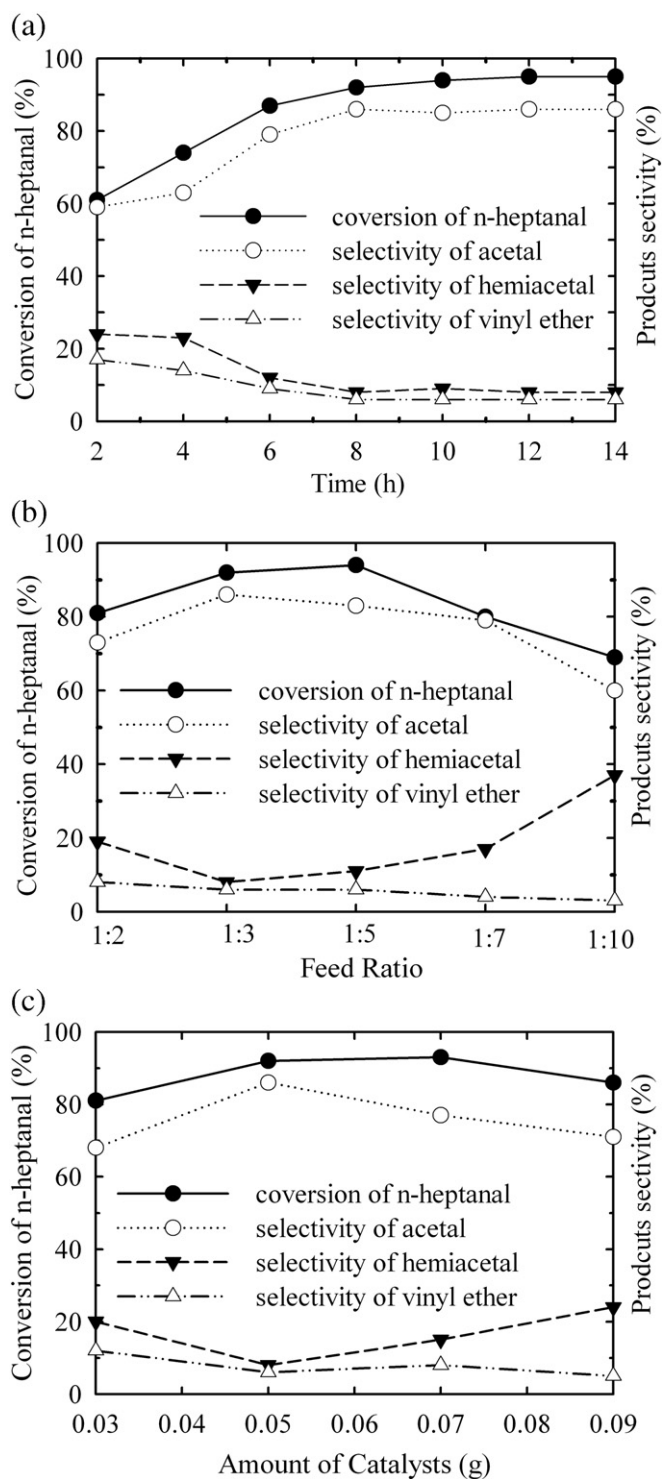
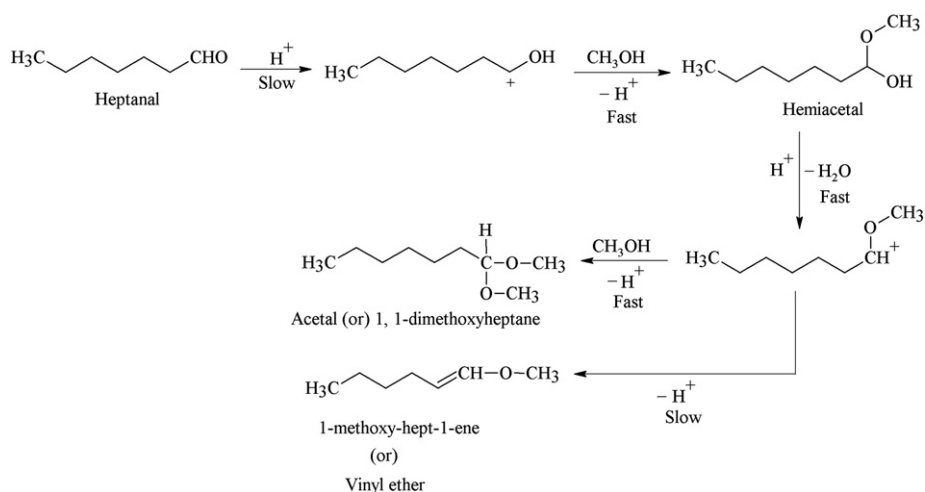


Fig. 5. Catalytic studies of acetalization of *n*-heptanal (a) effect of time, (b) effect of feed ratio and (c) effect of the amount of catalysts on *n*-heptanal conversion and products selectivity.

optimum feed ratio is 1:3. The slight increase in *n*-heptanal conversion at 1:5 and a subsequent decrease at 1:7 and 1:10 are due to *n*-heptanal dilution by excess methanol. The selectivity of hemiacetal increased slightly with an increase in the content of methanol in the feed above 1:3. This is attributed to the dilution of hemiacetal by excess methanol. The selectivity of acetal, therefore, increased from 1:2 to 1:3 and decreased thereafter. All these observations are in support of the proposed reaction pathway shown in Scheme 1.



Scheme 1. Possible pathway for the formation of hemiacetal, acetal and vinyl ether.

3.6.4. Effect of catalyst loading

The effect of catalyst loading on *n*-heptanal conversion and the products' selectivity was studied and the results are presented in Fig. 5c. The optimum catalyst loading was found to be 0.05 g. Since the feed ratio was 1:3, methanol content around the active site need not be the same with an increase in the catalyst amount and hence conversion decreased at higher loading. The selectivity of hemiacetal clearly demonstrates the existence of unequal distribution of methanol close to acid sites. The selectivity of acetal increased from 0.03 to 0.05 g of the catalyst but decreased at higher loading.

4. Conclusion

This study concluded that SBA-1 catalysts exhibited similar *n*-heptanal conversion irrespective of Si/Al and Si/(Al + Mg) ratios. This conclusion elucidated that the reaction is mainly controlled by their hydrophilic-hydrophobic property and free diffusion of reactants and products rather the acidity of the catalysts. This study also revealed that mesoporous materials are better than microporous materials for acetalization of long-chain aldehydes due to free diffusion in the mesoporous materials. This is a clean one-pot synthesis route for acetal compared to mineral acid-catalyzed route.

Acknowledgement

The authors gratefully acknowledge the financial support from the Council of Scientific & Industrial Research (CSIR), Government of India, New Delhi, for this research work. One of the authors (Mr. K. Venkatachalam) is grateful to CSIR for the award of Senior Research Fellowship (SRF).

References

- [1] L.F. Tietze, Chem. Rev. 96 (1996) 115–136.
- [2] T.W. Green, P.G.M. Wuts, 2nd ed., Protective Groups on Organic Synthesis, vol. 4, Wiley, New York, 1991, p. 212.
- [3] M.J. Climent, A. Vely, A. Corma, Green Chem. 4 (2002) 565–569.
- [4] K. Bauer, D. Garbe, H. Surburg, Common Fragrances and Flavour Materials, 2nd ed. VCH, New York, 1990.
- [5] D.M. Clode, Chem. Rev. 79 (1979) 491–513.
- [6] S.V. Ley, H.W.M. Priepeke, Angew. Chem. 106 (1994) 2412–2414.
- [7] M.K. Cheung, N.L. Douglas, B. Hinzen, S.V. Ley, X. Pannecoucke, Synlett, 1997, pp. 257–260.
- [8] K. Narasaka, M. Inone, T. Yamada, J. Sugiomori, N. Iwasawa, Chem. Lett. (1987) 2409–2412.
- [9] J.R. Bull, J. Floor, G.J. Kruger, J. Chem. Res. Synop. (1979) 224.
- [10] K. Bruns, J. Conard, A. Steigel, Tetrahedron 35 (1979) 2523–2530.
- [11] A.J. Elliot (Ed.), 1,3-Dioxalane Polymers in Comprehensive Heterocyclic Polymers, 6, Pergamon Press, Oxford, UK, 1984.
- [12] C.A. Mcckinzie, J.H. Stocker, J. Org. Chem. 20 (1955) 1695–1701.
- [13] J. Bornstein, S.F. Bedell, P.E. Drummond, C.F. Kosolowski, J. Am. Chem. Soc. 78 (1956) 83–86.
- [14] C.H. Lin, S.D. Lin, Y.H. Yang, T.P. Lin, Catal. Lett. 73 (2001) 2–4.
- [15] J.I. Tateiwa, H. Horiuchi, S. Uemora, J. Org. Chem. 60 (1995) 4039–4043.
- [16] F. Algarre, A. Corma, H. Garcia, J. Primo, Appl. Catal., A 128 (1995) 119–126.
- [17] M.J. Climent, A. Corma, S. Iborra, M.C. Navarro, J. Primo, J. Catal. 161 (1996) 783–789.
- [18] Y. Tanaka, N. Sawamura, M. Iwamoto, Tetrahedron Lett. 39 (1998) 9457–9460.
- [19] B. Thomas, S. Prathapan, S. Sugunan, Micropor. Mesopor. Mater. 80 (2005) 65–72.
- [20] A. Vinu, V. Murugesan, Martin Hartmann, Chem. Mater. 15 (2003) 1385–1393.
- [21] Q. Huo, D.I. Margolese, U. Ciesla, D.G. Demuth, P. Feng, T.E. Gier, P. Sieger, A. Firouzi, B.F. Chmelka, F. Schuth, G.D. Stucky, Chem. Mater. 6 (1994) 1176–1191.
- [22] Q. Huo, D.I. Margolese, G.D. Stucky, Chem. Mater. 8 (1996) 1147–1160.
- [23] L.X. Dai, K. Tabata, E. Suzuki, J. Mater. Sci. Lett. 19 (2000) 2071–2073.
- [24] S. Che, Y. Sakamoto, H. Yoshitake, O. Terasaki, T. Tatsumi, J. Phys. Chem. B 105 (2001) 10565–10572.
- [25] V.V. Balasubramanian, C. Anand, R.R. Pal, T. Mori, W. Bohlmann, K. Ariga, A.K. Tyagi, A. Vinu, Micropor. Mesopor. Mater. 121 (2009) 18–25.
- [26] B. Rabin dran Jermy, A. Pandurangan, J. Mol. Catal. A: Chem. 256 (2006) 184–192.